



Published in final edited form as:

J Med Chem. 2009 March 26; 52(6): 1639–1647. doi:10.1021/jm801313t.

Rational Modification of a Candidate Cancer Drug for Use Against Chagas Disease

James M Kraus¹, Christophe LMJ Verlinde², Mandana Karimi³, Galina I. Lepesheva⁴, Michael H Gelb^{1,2,*}, and Frederick S. Buckner^{3,*}

¹Department of Chemistry, University of Washington, Seattle, Washington 98195–7185, USA

²Department of Biochemistry, University of Washington, Seattle, Washington 98195–7185, USA

³Department of Medicine, University of Washington, Seattle, Washington 98195–7185, USA

⁴Department of Biochemistry, Vanderbilt University School of Medicine Nashville, TN, 37232–0146

Abstract

Chagas disease is one of the major neglected diseases of the world. Existing drug therapies are limited, ineffective and highly toxic. We describe a novel strategy of drug discovery of adapting an existing clinical compound with excellent pharmaceutical properties to target a pathogenic organism. The protein farnesyltransferase (PFT) inhibitor tipifarnib, now in phase III anti-cancer clinical trials, was previously found to kill *Trypanosoma cruzi* by blocking sterol 14 α -demethylase (14DM). We rationally developed tipifarnib analogs that display reduced affinity for human PFT to reduce toxicity, while increasing affinity for parasite 14DM. The lead compound has picomolar activity against cultured *T. cruzi* and is efficacious in a mouse model of acute Chagas disease.

Introduction

Chemotherapy for Chagas disease remains inadequate 100 years after the discovery of the etiologic agent, *Trypanosoma cruzi* (*T. cruzi*). This disease is responsible for approximately 21,000 deaths per year mainly in Latin America. The only drugs accepted for clinical use are the two nitroheterocyclic compounds, benznidazole and nifurtimox, which are inadequate due to toxicity and low cure rates during the chronic stage of the disease. The lack of pharmaceutical company interest for developing anti-*T. cruzi* drugs makes Chagas one of the major “neglected” diseases of the world. Our group has pursued a strategy of “piggyback” drug discovery in which we have attempted to identify compounds for Chagas disease that are well along in clinical development for other applications. We previously reported that the PFT inhibitor tipifarnib, in Phase III clinical trials for cancer, has potent activity against *T. cruzi* *in vitro* (EC₅₀ = 4 nM) despite having weak activity against the isolated *T. cruzi* PFT enzyme¹. Surprisingly, this compound inhibited the production of endogenous sterols in *T. cruzi* by binding to *T. cruzi* 14DM. Since tipifarnib and other PFT inhibitors have dose limiting toxicities in humans

Correspondences on biology should be addressed to FSB. Phone: (206) 598–9148, Fax: (206) 598–8819, Email: E-mail: fbuckner@u.washington.edu, Division of Allergy and Infectious Disease, Department of Medicine, University of Washington, Campus Box 357185, Seattle WA 98195–7185. Correspondences on chemistry should be addressed to MHG. Phone: (206) 543–7142, Fax: (206) 685–8665, Email: E-mail: gelb@chem.washington.edu, Address: Departments of Chemistry and Biochemistry, University of Washington, Campus Box 351700, Seattle WA 98195–1700.

*Contributed equally

Supporting Information Available.

Binding of key compounds to *T. cruzi* and human Lanosterol 14 α -Demethylase was assayed. This information along with an HPLC chromatogram of compound 2g is included in the Supplementary Material in the Supporting Information Section. This information is available free of charge via the Internet at <http://www.pubs.acs.org>

(particularly bone marrow suppression²) and since tipifarnib mediates its anti-*T. cruzi* effects by a mechanism other than blocking PFT, we directed our efforts toward the modification of the molecule in order to reduce its PFT inhibition activity and thereby eliminate a class-associated side effect.

Tipifarnib has characteristics that make it a desirable starting point for the development of an anti-Chagas drug. First, it is orally available with a long (16 hour) terminal half-life³. In cancer trials, tipifarnib is usually administered by pill twice per day. Since the majority of Chagas patients reside in resource limited settings, it is desirable that the drug be given orally. Furthermore, due to the nature of the infection (chronic tissue parasitism with a slowly dividing organism), a long course of therapy lasting weeks is likely to be necessary, which realistically can only be done with drugs administered orally. Second, tipifarnib has very little inhibitory activity against mammalian cytochrome P450 enzymes⁴. This is important since other 14DM inhibitors, such as ketoconazole, are fraught with problems due to inhibition of hepatic and adrenal P450 enzymes. Third, tipifarnib can be synthesized in eight steps from inexpensive starting materials, resulting in relatively low manufacturing costs. In contrast, posaconazole, which has also been studied as a potential anti-Chagas drug⁵, requires a synthesis of at least 16 steps⁶⁻⁸.

The crystal structure of human PFT bound to tipifarnib and farnesyl diphosphate [PDB 1SA4]⁹ guided our chemistry effort to abrogate the PFT inhibition activity of this compound. We looked for small changes in tipifarnib that would disrupt PFT binding while likely minimizing the impact on the pharmacologic properties of the molecule. Of course, it was necessary to make modifications that would be tolerated for interaction with the desired biological target, *T. cruzi* 14DM. Since a crystal structure for this enzyme has not been reported, predictions were made using a homology model based on the *Mycobacterium tuberculosis* CYP51 structure^{1, 10}. The compounds were tested for *in vitro* activity against rat PFT and against cultures of *T. cruzi* amastigotes (Table I).

Chemistry

The compounds were synthesized using modified published procedures¹¹⁻¹⁵. The synthesis affords a racemic final product and our analogs were tested as the racemic mixture. Tipifarnib as tested is enantiomerically pure, the enantiomers being resolved either by chiral chromatography or crystallization as diastereomeric salts. There are at least two main routes to compound **1** and its analogs **2a-g**. We followed a route that utilized a lithium-bromine exchange to generate a quinolin-6-yl anion nucleophile from a 6-bromo-2-methoxy-4-phenylquinoline **6a-g** to couple to an imidazol-5-yl-phenylmethanone **11a-c**¹⁵ (see Scheme Ia). The alternative method (not depicted) utilizes a modified Skraup-type quinoline synthesis involving cyclization of a cinnamoylanilide followed by C-6 benzylation and subsequent coupling of imidazole via organolithium species^{11, 13, 14}. We chose the former convergent synthetic strategy because it promised to make the modifications we were interested in easier to access. The first proposed analogs (compounds **2a** and **2b**) had modifications to Ring 1 of the scaffold (See Figure I) and the requisite substituted benzoic acid precursors were commercially available. Initially we expected to pursue more analogs containing modification at Ring 1 and a range of substituted benzoic acids was available. All were predicted to afford the requisite Weinreb amide via nucleophilic addition-elimination of the acid chloride in high yield, whereas it was not clear that all conceivable benzoic acids would have the same reactivity in the benzylation step of the Skraup method. Additionally, the method utilizing the Skraup cyclization required making the bond between the imidazole and the 6-benzoylquinoline via nucleophilic attack by *in situ* generated C-2 protected imidazol-5-yl anion nucleophile. Isomerization of the *in situ* generated imidazole is possible and was reported¹¹. We predicted that these isomers (C-5 linked imidazole product and C-2 linked imidazole side product) would

be difficult to separate. The imidazol-5-ylphenyl methanone intermediate **11a-c** was synthesized according to the published procedure¹⁵. The requisite benzoic acid precursor was converted to a benzoyl chloride, which upon reaction with *N,O*-dimethylhydroxylamine hydrochloride in the presence of base gives the Weinreb amide. Coupling to the *in situ* generated C-2 protected *N*-methylimidazol-5-yl anion gives the methanone intermediate **11a-c** on aqueous workup with 1N HCl. See Scheme Ib

For compounds **2a,b** the 6-bromomethoxyquinoline intermediates **6a,b** were formed via a condensation of phenylacetonitrile with nitrobenzene to form a 3-phenyl-2,1-benzisoxazole **3a,b** which was then converted to **4a,b** by reductive ring opening with aqueous TiCl₃/HCl^{11, 15}. We became interested in substitution of the *ortho* position of the 3-phenyl ring as a result of molecular modeling studies, compound **2c**. The requisite intermediate isoxazole **3c** had been reported via condensation of (2-methylphenyl)acetonitrile and nitrobenzene in 54% yield¹⁶. At the time, the needed phenylacetonitrile **19c** was not commercially available. Intermediate **19c** was simple to prepare in three steps using reported conditions for reduction of benzoic acid to benzyl alcohol¹⁷, conversion of the benzyl alcohol to benzyl bromide¹⁸, and substitution of bromide to cyanide¹⁹. (See Scheme II) Unfortunately we were never able to reproduce the reported 54% yield for the condensation reaction and in our hands the yield hovered at around 10%. We were very interested in this compound from a modeling standpoint so we pushed the required material through the dismal 10% yield. Upon testing of the new analog **2c** we were very pleased to discover that our docking prediction was true, the installation of a simple methyl group significantly knocked down PFT affinity (around 420 fold), see discussion for details. This exciting activity led us to **2d**, which had even slightly higher selectivity, being about 430 times worse on PFT than tipifarnib. We concluded that we would like to evaluate the pharmacokinetics of these compounds in our mouse model. This required approximately 6–7 mg of product and it did not make sense to prepare this much material via the low yielding route. We therefore sought an easier route to intermediate **4**. There are a multitude of routes to synthesize *ortho*-aminobenzophenones²⁰. Conversion of isatoic anhydride to *ortho*-aminobenzophenone had been previously reported¹². We speculated that 5-bromoisatoic anhydride could be similarly converted to the corresponding 5-bromo-2-aminobenzophenone **4c** in one step using organolithium species. We modified the protocol, using a strategy of inverse addition with 2 equivalents of *in situ* generated phenyllithium to obtain intermediate **4c** in yield 71% overall yield from 5-bromoisatoic anhydride. (See Scheme III). Compounds **2a-f** were formed from intermediate **9** by substitution of alkyl chloride by gaseous ammonia. Our lead compound **2g** was formed from **9** via an acid catalyzed dehydration/etherification in methanol as solvent. It had previously been reported that higher molecular weight alcohols could be converted to the trityl type ether using catalytic amounts of *p*-toluenesulfonic acid and a Dean-Stark apparatus utilizing the benzene-water azeotrope to remove water²¹. We simply dissolved the starting material in methanol and heated to reflux in the presence of catalytic amounts of tosic acid. This led to conversion of **9** to **2g** in 75% isolated yield on the gram scale. All of the analogs that we prepared are racemates. Our plan is to go forward with pre-clinical development of these compounds as racemates.

Results and Discussion

Molecular modeling suggested that modifications to ring-1 (Fig. I) would partially displace tipifarnib from the PFT active site. When tested, the addition of a 3-methyl to the tipifarnib ring-1, compound **2a**, gave rise to a 19-fold increase in IC₅₀ (to 13 nM) on rat PFT compared to tipifarnib. A slightly larger effect on PFT inhibition (IC₅₀ 17 nM) was observed by substituting a naphthyl group at the ring-1 position in compound **2b**. These initial analogs showed the desired trend, but the decrease in PFT inhibition was accompanied by a decrease in activity against the parasites. To achieve the desired result, we next explored modifications on ring-2 of tipifarnib (Fig. I). Introduction of a 2-methyl group on this ring (**2c**) was predicted

to be detrimental for binding to human PFT by causing steric clash with the molecular surface of the binding pocket (Fig. IIa). Ring-2 of tipifarnib points to a hydrophobic pocket near the entrance to the active site in the 14DM model. We predicted that tipifarnib does not fill this pocket, leaving room for a methyl group (**2c**, Fig. IIb). Specifically, compound **2c** displays a 420-fold decrease in PFT inhibition with an IC_{50} of 294 nM on mammalian PFT and only minor reduction in activity against *T. cruzi* amastigotes. A more substantial change of replacing the tipifarnib ring-2 with a naphthyl group in **2f** further knocked down PFT inhibition (IC_{50} 485 nM), while retaining anti-*T. cruzi* activity. All along we adhered to a “piggy back” strategy, using a philosophy that smaller changes would be better, if made in the right places, since the parent compound, compound **1** had excellent pharmaceutical properties to begin with and big changes might have a big effect on pharmacokinetics or toxicity. Since compound **2c** had such high selectivity from the installation of simple methyl group, we decided to proceed with this basic structure.

The amino group of tipifarnib makes a water-mediated H-bond to a phosphate oxygen of farnesyl diphosphate in the active site of mammalian PFT⁹. Our homology model of *T. cruzi* demethylase predicted that H-bonding to this amino group is not important for binding in 14DM¹, so we substituted NH_2 for OMe to arrive at **2g**. Relative to tipifarnib, this compound resulted in a ~10-fold increase in potency against *T. cruzi* amastigotes while having further reduced activity against PFT ($IC_{50} > 5,000$ nM). We speculate that this improved cellular activity may be due to increased affinity for 14DM or increased cellular permeability. Using recombinant *T. cruzi* 14DM reconstituted *in vitro* with P450 reductase, we showed that **2c**, **2f** and **2g** bind to Tc14DM with equilibrium dissociation constants much less than minimum concentration of the enzyme required in the assay (1 μM , see Supplementary Information). In the same conditions tipifarnib, **2c**, **2f**, and **2g** do not inhibit the human 14DM (see Supplementary Information).

The potency of **2g** against *T. cruzi* cultures puts it in the same league as the most potent (antifungal) azoles, ketoconazole and posaconazole (Table I). Therefore, we moved ahead with **2g** as the lead for additional *in vivo* studies beginning with pharmacokinetic studies in mice. Fig. IIIa shows that **2g** has a very similar pharmacokinetic profile to tipifarnib in mice, with peak serum concentrations (C_{max}) of 5–7 μM and an elimination half-life ($T_{1/2}$) of ~4 hrs. Based on these results, we designed an efficacy study using **2g** in a mouse model of Chagas disease (Fig. IIIb). In this model, a parasite infection is first established for 7 days and then **2g** is administered by oral gavage over a 20 day period (see Supplementary Information). Control mice given only the Vehicle developed steadily rising parasitemia and death by day 16 post-infection. Compound **2g** suppressed parasitemia to microscopically undetectable levels, similar to the effect of the control drug benznidazole. Interestingly, tipifarnib only delayed the development of high parasitemia by 3–4 days and did not protect the mice from death. This is probably due to the 10-fold lower potency of tipifarnib on *T. cruzi* compared to **2g**, but it could also be related to other factors such as tissue distribution of the compounds. One mouse in the **2g** group died after the end of treatment. This was not due to inadequate parasitologic clearance, but appeared to be related to a physical complication from receiving multiple gavage treatments. The other four mice in the group remained healthy and did not experience apparent adverse effects from the **2g** treatment. The benznidazole treated mice also tolerated the treatment without apparent adverse effects. At 100 days post-infection, parasites were microscopically undetectable in the blood. At day 103, the mice were sacrificed, exsanguinated and blood cultures were set up to test for parasitologic cure. All 4 surviving **2g**-treated mice had positive parasite blood cultures and 3 of 6 benznidazole-treated mice had positive blood cultures. This indicates that neither compound was completely curative using this treatment regimen. There are numerous animal models of the disease in the literature involving different strains of *T. cruzi* as well as various drug dosing schedules and timelines^{5, 22-26}. We chose the model involving dosing for 20 days because it is so widely used^{5, 22, 23},

^{25, 26}. As with other chronic infections, it is possible that combination chemotherapy may be necessary to completely eliminate *T. cruzi* from the human host.

The tipifarnib analogs display poor inhibition of the hepatic cytochrome P450 enzyme, CYP3A4, compared to the azole antifungal drugs (Table I). This indicates that the tipifarnib analogs are likely to produce fewer problems with drug-drug interactions than the azole class of anti-fungal drugs, which have also been investigated as anti-*T. cruzi* agents via inhibition of sterol 14 α -demethylase.

The new tipifarnib analogs were shown to have low cytotoxicity against a panel of mammalian cells with EC₅₀ values >5 μ M for all compounds against five different types of cell lines (data not shown).

The best compound, **2g**, did not have apparent toxicity in mice when dosed at 50 mg/kg twice per day. This compound also appears to retain the desirable properties of tipifarnib in terms of a good pharmacokinetic profile when administered orally (in mice) and demonstrating weak inhibition of the human CYP3A4 enzyme *in vitro*.

Conclusions

We describe a novel strategy of drug discovery in which we modified an existing clinical cancer compound with excellent pharmaceutical properties, compound **1**, to use as an anti-parasitic. We previously discovered that this compound has activity against two enzymes, an off-target human PFT enzyme and *T. cruzi* Lanosterol 14 α -demethylase. Small changes to the structure of compound **1** led to complete elimination of PFT inhibitory activity and simultaneously increased activity against *T. cruzi*. Our best compound, **2g**, is orally available, inexpensive to produce and extremely potent, showing activity at picomolar concentrations *in vitro*. In a mouse model of the disease, **2g** showed complete suppression of parasitemia, microscopically, and efficacy comparable to the principle clinical therapeutic, benznidazole, which has toxic side effects. Removal of the PFT inhibitory activity in this group of compounds is expected to eliminate class-associated side effects inherent to PFT inhibitors. **2g** is one of the most potent *T. cruzi* compounds ever reported and we are optimistic that a compound such as **2g** is extremely promising for further development as a clinical candidate for Chagas disease.

Experimental Methods

Molecular Modeling

We made use of the crystal structure of Rat PFT in complex with tipifarnib⁹ and the homology model of the *T. cruzi* CYP51 in complex with tipifarnib, based on the *Mycobacterium tuberculosis* enzyme structure, described earlier in detail¹, for all molecular modeling. Design and docking studies were carried out with the FLO/QXP program suite, version 0602²⁷. In each case amino acid residues within 11 Å of tipifarnib were included in the binding site model for Metropolis Monte Carlo searches and energy minimization procedures. Details of the procedures were earlier described for human PFT¹. Figures of structural models were created using PyMOL (www.pymol.org).

PFT enzyme assay

Expression and purification of recombinant rat PFT in *Sf9* cells was reported previously²⁸. Compounds were screened against rat PFT by a ³H-Scintillation Proximity Assay (SPA; TRKQ7010; Amersham Biosciences Corp., Piscataway, NJ). The experiments were performed as described elsewhere²⁹ with the following modifications. Rat PFT assays were carried out in buffer (pH 7.5, 50 mM HEPES, 30 mM MgCl₂, 20 mM KCl, 5 mM dithiothreitol, 0.01% Triton X-100), 1 μ M human lamin B carboxy-terminus peptide (biotin-YRASNRSCAIM), and

1 μCi [^3H]farnesyl diphosphate (15 to 20 Ci/mmol; Amersham) in a total volume of 50 μL which included 1 μL of PFT inhibitor solution in dimethylsulfoxide (DMSO) and 10 ng of purified rat PFT. The reaction mixtures were incubated at 37°C for 60 min and terminated by addition of 70 μL of assay STOP solution (Amersham) and 5 μL SPA beads. The assay mixture was incubated at room temperature for 30 min. The assay results were counted on a Chameleon 425–104 multilabel plate counter (Hidex Oy) that detected the photons emitted by the scintillation beads bound to biotin-peptide- ^3H farnesyl. The inhibitor concentration that caused 50% PFT inhibition (IC_{50}) was determined by non-linear regression analysis of a plot of percent enzyme inhibition versus log of inhibitor concentration. Curves were fit to a variable slope sigmoidal dose-response curve using GraphPad Prism 3.0 (www.graphpad.com).

T. cruzi growth inhibition assay

Compounds were screened against the β -galactosidase expressing Tulahuen strain of *T. cruzi* in 96 well tissue culture plates as described previously³⁰.

Mammalian cell growth inhibition assays

Compounds were screened for cytotoxicity against five different mammalian cell lines representing different tissue types: HT-1080 (human fibrosarcoma), SF-539 (human neural cells), HCC-2998 (human adenocarcinoma), THP-1 (human macrophage), and CRL-8155 (human lymphocyte). All cell lines were purchased from American Tissue Culture Collection. Cells were grown in the presence of compounds for 48 hours before growth was quantified using Alamar Blue (Alamar Biosciences Inc., Sacramento, CA). Compounds were tested at final concentrations of 25, 12.5, 6.25, 3.13, 1.56, and 0.78 μM .

CYP3A4 inhibition assay

Inhibition of recombinant human CYP3A4 enzyme was determined using a commercial kit (CYP3A4/BFC High Throughput Inhibitor Screening Kit) following the manufacturer's instructions (GenTest, Inc.).

Pharmacokinetic studies in mice

Compounds were suspended at 10 mg/ml in 20% (w/v) Trappsol™ hydroxypropyl beta-cyclodextrin (pharmaceutical grade) (CTD, Inc.) and administered to BALB/c mice (7–8 week females weighing approximately 20 g) by oral gavage in a volume of 100 μL . Thus, the mice received a dose of 50 mg/kg. At timed intervals, 40 μL of tail blood was collected in heparinized capillary tubes. Plasma was separated by centrifugation and frozen for later analysis. After thawing, 10 μL of plasma was mixed with 11 μL of acetonitrile containing 100 pmols compound **2e** as an internal standard. The mixture was vortexed, then mixed with 30 μL extraction solvent composed of 80% acetonitrile and 20% H_2O by volume. This was centrifuged at 13,200 rpm for 10 minutes at which time most of the supernatant was transferred to a new tube and dried down to a solid. To determine response factors, 10 μL of fresh plasma (containing no drug) was obtained and spiked with 100 pmols of analyte then mixed with 11 μL acetonitrile containing 100 pmols of compound **2e**. This was similarly vortexed, mixed with 30 μL extraction solvent, centrifuged at 13,200 rpm for 10 minutes at which time most of the supernatant was transferred to a new tube and dried down to a solid. Samples were reconstituted in 50 μL of a mixture of 50% acetonitrile and 50% water by volume. Concentrations were determined by liquid chromatography-mass spectrometry using an Agilent (Palo Alto, CA) HP 1100 chromatograph and an Esquire-LC (Bruker, Billerica, MA) electrospray ion trap mass spectrometer. Reversed-phase LC separation was performed using an Agilent Zorbax SB-C18 (3.5 μm , 2.1 mm \times 100 mm) with a mobile phase consisting of water/5% acetonitrile/1% acetic acid (solvent A) and acetonitrile/1% acetic acid (solvent B). Mobile phase gradient went from 10% solvent B to 64% solvent B over 9 minutes with a flow

rate of 0.2 mL/min, then flow rate was increased to 0.35 mL/min with a gradient from 64% solvent B to 100% over 5 minutes. Compounds were quantified by integration of the area of each peak in an extracted ion chromatogram. Quantification was performed with Bruker QUANTANALYSIS software using response factors established for the internal standard.

Efficacy studies in mice

BALB/c mice (7–8 week females) were infected with 5×10^3 *T. cruzi* trypomastigotes (Tulahuen strain) by subcutaneous injection. By 7 days post-infection, every mouse had microscopically observable parasites on slides of peripheral blood. On day 8 post-infection, mice (in groups of 5 or 6) began receiving treatments by oral gavage. For tipifarnib and **2g**, mice were initially dosed at 100 mg/kg twice per day (days 8–13), but some weight loss was observed, so the dose was reduced to 50 mg/kg twice per day for days 14–27. The benzimidazole group received this drug at 100 mg/kg once per day (days 8–27). The control group received the vehicle (20% (w/v) Trappsol™ hydroxypropyl beta-cyclodextrin (pharmaceutical grade) (CTD, Inc.)), in a volume of 100 μ L twice per day. Parasitemia was monitored by placing 5 μ L of tail blood under a cover slip and counting 50 high-powered fields. Mice that were pre-morbid from progressive infection were euthanized. All surviving mice were sacrificed on day 103 post-infection and \sim 500 μ L of blood from cardiac puncture was taken for culture in liver-infusion tryptone medium plus 10% heat-inactivated fetal bovine serum, penicillin, and streptomycin³¹. The culture was incubated at 28° C and checked weekly (for 8 weeks) for outgrowth of *T. cruzi* epimastigotes.

Chemistry

Starting materials were purchased from Aldrich, Acros, Alfa-Aesar, EMD, Fisher, Lancaster, Mallinckrodt, TCI-America, or VWR and used without further purification, unless otherwise specified. *N*-methylimidazole (M50834) was purchased from Sigma-Aldrich and distilled at reduced pressure (10mm Hg, bp: 67–69 °C) after being stirred over sodium at room temperature overnight. Solvents were purified using a J.C. Meyer type Solvent Dispensing System utilizing Al₂O₃ and/or Copper cartridges, depending on the particular solvent. Nitrogen gas used in reactions requiring an inert atmosphere was house supplied nitrogen run through Dry-Rite dessicant. Glassware for distillation and critical reactions was flame dried under vacuum or dried in an oven. Silica was EMD Silica Gel 60, 40–63 μ m (11567–1). TLC plates were aluminum backed EMD Silica Gel 60 F₂₅₄ (5554/7). NMR spectra were recorded on a Bruker Avance AV300. ESI-MS were recorded on a Bruker Esquire Ion Trap Mass Spectrometer. The synthesis of compound **2g** is described and compounds **2a-f** were prepared in an analogous fashion using the corresponding commercially available starting materials. Purification of final compounds was by reverse phase HPLC utilizing octadecylsilane stationary phase and a water-to-methanol gradient with 0.08% v/v Trifluoroacetic Acid, (TFA). HPLC was a Varian Pro-Star fitted with YMC Pack-ODS-A 2 \times 10 cm column running at 12 mL/min using an excitation wavelength of 254 nm. All tested target compounds possessed a purity of \geq 95% as verified by HPLC.

2-Amino-5-bromo-*N*-methoxy-*N*-methylbenzamide (**3**)

A 2 L flask was charged with 10.0 g (41.3 mmols) 5-bromoisatoic anhydride (242.03 g/mol) and 6.0 g (61.5 mmols) *N,O*-dimethylhydroxylamine hydrochloride (97.54 g/mol). The solids were suspended in 150 mL anhydrous CH₂Cl₂ and stirred rapidly. 15.0 mL pyridine (186 mmol) was added slowly and mixture was allowed to stir overnight. The crude mixture was partitioned between CHCl₃ and water. The organic phase was washed with brine and dried with anhydrous MgSO₄. Solvents were removed under reduced pressure to produce a golden colored oil which crystallized upon standing. Product was triturated with hexanes, filtered then used without further purification. 8.3 g lightly colored crystalline **3** was produced, 83%

yield. ^1H NMR (300 MHz, CDCl_3 , δ): 7.52 (d, $J = 2.4$ Hz, 1H), 7.28 (dd, $J = 2.4$ Hz, 8.1Hz 1H), 6.61 (d, $J = 8.7$ Hz, 1H), 4.69 (s (broad), 2H), 3.61 (s, 3H), 3.36 (s, 3H) ESI-MS m/z 283.1 ($\text{M} + \text{Na}^+$) $^+$ MW: 259.10 g/mol.

(2-Amino-5-bromophenyl)(3-chloro-2-methylphenyl)methanone (4g)

A 250 mL flask was flame dried, charged with a stirbar and sealed with a new rubber septum. 2-Bromo-6-chlorotoluene (6 mL, 45.9 mmols) was added to the flask and dissolved in 60 mL of anhydrous THF under an atmosphere of dry nitrogen. The solution was stirred for about 5 minutes and then cooled to -78 °C with a dry ice acetone bath, then stirred for about 10 minutes. 18 mL (45.9 mmols, 1 eq.) *n*-butyllithium (2.5 M in hexanes) was added dropwise at a rate such that temperature of the reaction remained close to -78 °C, as indicated by the slow sublimation of CO_2 . The solution was allowed to stir for 20 minutes. A separate flask was flame dried and fitted with a stir-bar and septum. 5.95 g (22.95 mmols, 0.5 eq) 2-amino-5-bromo-*N*-methoxy-*N*-methylbenzamide **3** was added and dissolved in 60 mL anhydrous THF. After stirring for about 5 minutes, this solution was transferred drop-wise by cannula to the flask containing the in situ generated aryllithium. The solution was allowed to stir at this temperature for 2 hours at which time the cooling bath was removed allowing the flask to rise to room temperature. 50 mL 1 M aqueous HCl was added and the bi-phasic mixture was allowed to stir for 30 minutes. Crude product was partitioned between CHCl_3 and water. The organic phase was washed three times with saturated, aqueous NaHCO_3 , then separated and dried with MgSO_4 . Solvents were removed under reduced pressure to produce an orange-brown colored oil. This was purified on silica with 20% EtOAc/hexanes to produce 6.3 g of yellow crystalline **4g**, yield 85%. ^1H NMR (300 MHz, CDCl_3 , δ): 7.47 (d, $J = 7.8$ Hz, 1H), 7.36 (dd, $J = 8.7$ Hz, 2.1Hz, 1H), 7.25 (d, $J = 2.1$ Hz 1H), 7.21 (m, 2H), 7.11 (d, $J = 7.5$ Hz 1H), 6.64 (d, $J = 8.7$ Hz, 1H), 6.49 (s (broad), 2H), 2.27 (s, 3H) ESI-MS m/z 324.3 ($\text{M} + \text{H}^+$) $^+$ MW: 324.60g/mol.

6-Bromo-4-(3-chloro-2-methylphenyl)quinolin-2(1H)-one (5g)

A 250 mL flask was fitted with a stir-bar and 11.9 g of **4g**. A water condenser was attached. 50 mL anhydrous toluene was added and 24.3 mL (257 mmols, 7 eq.) acetic anhydride was added dropwise, rapidly. The solution was heated to reflux for 6 hours at which time the volatiles were removed under reduced pressure. Toluene was added and removed at reduced pressure two more times. The crude product was set aside. A separate flask was fitted with a stir-bar and a septum and loaded with 24.7 g (220 mmols, 6 eq.) of 95% *t*BuOK powder. This was suspended in 120 mL 1,2-dimethoxyethane (DME) and stirred for about 10 minutes. The temperature was lowered to 0 °C. The crude product set aside previously was dissolved in 45 mL 1,2-dimethoxyethane then transferred drop-wise by cannula to the flask containing the *t*BuOK suspension. The color of the solution changed to yellow and the mixture was allowed to stir under an inert atmosphere overnight. DME solvent was removed at reduced pressure and the resulting paste was suspended in approximately 300 mL water. The solid was collected by filtration and used at the next step without purification. 8.4 g (24.10 mmols) of **5g** was produced as a fluffy, white solid, yield 66%. ^1H NMR (300 MHz, CDCl_3 , δ): 7.62 (dd, $J = 8.7$ Hz, 1.8Hz, 1H), 7.53 (d, $J = 7.8$ Hz, 1H), 7.39 (d, $J = 8.7$ Hz, 1H), 7.30 (m, 1H), 7.21 (d, $J = 1.8$ Hz, 1H), 7.11 (d, $J = 7.2$ Hz, 1H), 6.62 (s, 1H), 2.17 (s, 3H) ESI-MS m/z 348.3 ($\text{M} + \text{H}^+$) $^+$ MW: 348.62 g/mol.

6-Bromo-4-(3-chloro-2-methylphenyl)-2-methoxyquinoline (6g)

A flame dried 25 mL flask was fitted with a stir-bar and charged with 500 mg (1.43 mmols) of **5g** and 423 mg (2.86 mmols, 2 eq.) BF_4OME_3 then sealed with a septum. The solids were suspended in 5.5 mL of anhydrous CH_2Cl_2 and stirred for 20 hours at which time 5.5 mL of 1 M aqueous NaOH was added. The mixture was stirred for about 3 hours, then partitioned between CHCl_3 and water, organic was washed three times with brine, then dried with

MgSO₄. Solvents were removed under reduced pressure to produce a clear yellow oil which crystallized upon standing. This was purified on silica with 50:50 CH₂Cl₂:hexane to produce 329 mg of **6g** as a flaky yellow-green solid, yield 63%. ¹H NMR (300 MHz, CDCl₃, δ): 7.79 (d, *J* = 9.0 Hz, 1H), 7.69 (dd, *J* = 8.7Hz, 2.3Hz, 1H), 7.50 (dd, *J* = 7.8Hz, 1.2Hz, 1H), 7.40 (d, *J* = 2.1 Hz, 1H), 7.26 (m, 1H), 7.09 (dd, *J* = 7.5Hz, 1.2Hz, 1H), 6.77 (s, 1H), 4.10 (s, 3H), 2.08 (s, 3H) ESI-MS *m/z* 362.3 (M + H⁺)⁺ MW: 362.65 g/mol.

4-Chloro-*N*-methoxy-*N*-methylbenzamide (10)

20.0 g (0.128 mols) 4-chlorobenzoic acid (156.57 g/mol) was placed in a 500 mL round bottomed flask. 120 mL thionyl chloride was added and the mixture was refluxed overnight. Thionyl chloride was removed under reduced pressure to produce a red colored oil. Anhydrous toluene was added and then removed under reduced pressure two times. The crude product was dissolved in 200 mL anhydrous dichloromethane (DCM). 13.73 g (0.140 mols) *N,O*-dimethylhydroxylamine•HCl (97.54 g/mol) was added. 52 mL (0.640 mols) anhydrous pyridine was added over a period of 10 minutes. The reaction was stirred under nitrogen at room temperature overnight. Volatiles were removed under reduced pressure. Solid was partitioned between CHCl₃ and water. The organic phase was washed with brine, then collected and dried over anhydrous magnesium sulfate. The solvents were removed to produce a red colored oil which was purified on silica with 5% MeOH/CH₂Cl₂ as eluent. 22.9 g produced, yield 90%. ¹H NMR (300 MHz, CDCl₃, δ): 7.66 (d, *J* = 8.4 Hz, 2H), 7.38 (d, *J* = 8.4 Hz, 2H), 3.54 (s, 3H, -OMe), 3.36 (s, 3H, -NMe) ESI-MS *m/z* 200.4 (M + H⁺)⁺ MW: 199.63 g/mol.

(4-Chlorophenyl)(1-methyl-1H-imidazol-5-yl)methanone (11)

A flame dried 125 mL round bottom flask was charged with a stir bar, and over-pressurized with dry nitrogen gas and 3.0 mL (37.6 mmols) freshly distilled *N*-methylimidazole (82.11 g/mol, 1.035 g/mL). The flask was sealed with a new rubber septum and 30 mL anhydrous THF was added. The solution was stirred for about 10 minutes, and then the temperature was lowered to -78 °C and stirred for an additional 10 minutes. 16.2 mL (41.3mmols) freshly titrated *n*-butyl lithium (2.5 M in hexanes) was added drop-wise through the septum over a period of 10 minutes under an overpressure of dry nitrogen. A slight color change to pale yellow was observed. This was allowed to stir at this temperature for 45 minutes, then 6.3 mL (37.6 mmols) 99% chlorotriethylsilane (Et₃SiCl) was added drop-wise over 5 minutes. The reaction was allowed to stir for 1 hour at -78 °C, at which point 15.0 mL (37.6 mmols) freshly titrated *n*-butyl lithium (2.5 M in hexanes) was added drop-wise through the septum over a period of 10 minutes and allowed to stir at -78 °C for an additional 45 minutes. A separate flask was flame dried and charged with 5.0 g (25.1 mmols) Weinreb amide **10** (199.63 g/mol) and sealed. 15 mL anhydrous THF was added and the mixture was stirred at room temperature for 10 minutes, then at the appropriate time, transferred via cannula to the flask containing the in-situ generated C-2 triethylsilyl protected *N*-methylimidazole at a slow rate to maintain low temperature as indicated by the slow sublimation of CO₂. The mixture was left to stir overnight and became a deep red color. The reaction was quenched by the addition of 1 M HCl until the pH of the aqueous phase was no longer basic as indicated by litmus paper, then allowed to stir for one hour. The pH of the aqueous phase was adjusted to above 8 with 1.5 M NaOH and the mixture was partitioned between CHCl₃ and water. The organic phase was washed with brine and dried with anhydrous MgSO₄. Solvents were removed under reduced pressure to produce a reddish solid. Product was purified by re-crystallization from CH₂Cl₂ to produce 4.24 g fluffy golden crystals, 76.6% yield. ¹H NMR (300 MHz, CDCl₃, δ): 7.83 (d, *J* = 8.4 Hz, 2H), 7.68 (s, 1H), 7.59 (s, 1H), 7.50 (d, *J* = 8.4 Hz, 2H), 4.03 (s, 1H) ESI-MS *m/z* 221.4 (M + H⁺)⁺ MW: 220.65 g/mol.

4-(3-Chloro-2-methylphenyl)-6-((4-chlorophenyl)(hydroxy)(1-methyl-1H-imidazol-5-yl)methyl)-2-methoxyquinoline (7g)

A flame dried flask was charged with a stir bar, 4.2 g (11.58 mmols) of **6g** and sealed with a rubber septum. Solid was dissolved in 20 mL anhydrous THF was added and stirred at room temperature for 10 minutes. The temperature was lowered to $-78\text{ }^{\circ}\text{C}$, and stirred for another 10 minutes. 5.0 mL (1.1 eq. 6.369 mmols) 2.5 M n-butyllithium was added dropwise accompanied by a color shift to dark yellow-orange. This was allowed to stir for 20 minutes. A separate flask was flame dried and charged with 2.8 g **11c** (1.1 eq., 6.369 mmols). This was dissolved in 55 mL THF and added to the flask containing quinoline in three increments, rapidly drop-wise over 10 minutes. Color shifted steadily to yellow-gold after stirring overnight and warming slowly to room temperature. The reaction was quenched by addition of 1 volume equivalent of a saturated aqueous solution of NH_4Cl . This was partitioned between 1 M NH_4OH and CHCl_3 . Organic phase was collected and solvents were removed under reduced pressure to produce a foamy, white semi-solid. This was purified on silica with a mobile phase consisting of $\text{MeOH}/\text{CH}_2\text{Cl}_2$ 1:10 v/v to produce 3.52 g (6.91 mmols), 60% yield. TLC (CH_2Cl_2 : MeOH 9:1 v/v): $R_f = 0.45$; $^1\text{H NMR}$ (300 MHz, CDCl_3 , δ): 7.86 (m, 1H), 7.59 (m, 1H), 7.43 (m, 1H), 7.20 (m, 6H), 7.01 (m, 2H), 6.79 (s, 1H), 6.17 (m, 1H), 4.12 (s, 3H), 3.30 (m, 3H), 1.90 (m, 3H) ESI-MS m/z 504.3 ($\text{M} + \text{H}^+$)⁺ MW: 504.41 g/mol.

4-(3-Chloro-2-methylphenyl)-6-((4-chlorophenyl)(hydroxy)(1-methyl-1H-imidazol-5-yl)methyl)quinolin-2(1H)-one (8g)

3.5 g (6.91 mmols) **7g** was dissolved in 15 mL THF. 30 mL 6 N HCl (25 eq) was added dropwise. The flask was fitted with a water-cooled condenser and the mixture was stirred at $60\text{ }^{\circ}\text{C}$ for 5 hours. THF was removed by a stream of nitrogen and the homogenous organic phase was made basic with excess aqueous 1 M NH_4OH then extracted with CHCl_3 . The organic was collected and dried with MgSO_4 then solvents were removed at reduced pressure. Product was purified on silica with a mobile phase consisting of $\text{MeOH}/\text{CH}_2\text{Cl}_2$ 1:10 v/v to produce 2.1 g (4.28 mmols) of **8g** as a white solid, 62% yield. TLC (CH_2Cl_2 : MeOH 9:1 v/v): $R_f = 0.30$; $^1\text{H NMR}$ (300 MHz, CDCl_3 , δ): 7.68 (m, 1H), 7.59 (m, 1H), 7.47 (m, 2H), 7.28 (m, 3H), 7.12 (m, 3H), 6.73 (m, 1H), 6.51 (m, 1H), 6.1 (m, 1H), 3.41 (m, 3H), 1.96 (m, 3H) ESI-MS m/z 490.4 ($\text{M} + \text{H}^+$)⁺ MW: 490.38 g/mol.

4-(3-Chloro-2-methylphenyl)-6-((4-chlorophenyl)(hydroxy)(1-methyl-1H-imidazol-5-yl)methyl)-1-methylquinolin-2(1H)-one (9g)

2.1 g (4.28 mmols) **8g** was added to a 100 mL flask and dissolved in 30 mL THF. 487 mg (0.5 eq., 2.14 mmols) benzyltriethylammonium chloride was added as a phase transfer catalyst. 25.5 mL 40% wt. NaOH (120 eq., 17.1 g) was added and allowed to stir for approximately 10 minutes. 375 μL (1.4 eq., 6 mmols) CH_3I was added and the mixture was allowed to stir overnight. The THF was removed at reduced pressure and the product was partitioned between CHCl_3 and 1M NH_4OH . The product was purified on silica with a mobile phase consisting of $\text{MeOH}/\text{CH}_2\text{Cl}_2$ 1:10 v/v to produce 2.0 g (3.97 mmols) of **9g** as a colorless semi-solid, 59% yield. TLC (CH_2Cl_2 : MeOH 9:1 v/v): $R_f = 0.45$; $^1\text{H NMR}$ (300 MHz, CDCl_3 , δ): 7.80 (m, 1H), 7.72 (m, 1H), 7.63 (m, 1H), 7.49 (m, 1H), 7.29 (m, 3H), 7.12 (m, 3H), 6.78 (m, 1H), 6.58 (m, 1H), 6.14 (m, 1H), 3.85 (s, 3H), 3.41 (m, 3H), 1.95 (m, 3H) ESI-MS m/z 504.3 ($\text{M} + \text{H}^+$)⁺ MW: 504.41 g/mol.

4-(3-Chloro-2-methylphenyl)-6-((4-chlorophenyl)(methoxy)(1-methyl-1H-imidazol-5-yl)methyl)-1-methylquinolin-2(1H)-one (2g)

60.0 mg (0.119 mmols) **9g** was dissolved in 10 mL of MeOH and approximately 60 mg tosic acid was added. The reaction was heated to reflux for 48 hours. One spot by TLC. Solvents were removed under reduced pressure to produce a colorless, oily semi-solid. Product was

purified by HPLC using a water-methanol gradient with 0.08% v/v trifluoroacetic acid. 30–100% over 20 minutes followed by 10 minutes at 100%. Product elutes at 16.1 minutes. 56.5 mg (0.0893 mmols) produced as a mono-TFA salt. Yield 75%. TLC (CH₂Cl₂:MeOH 9:1 v/v): *R*_f = 0.55; ¹H NMR (300 MHz, CDCl₃, δ): 8.99 (m, 1H), 7.85 (m, 1H), 7.75 (m, 1H), 7.53 (m, 2H), 7.35 (m, 5H), 7.14 (m, 1H), 6.98 (m, 1H), 6.62 (s, 1H), 3.83 (s, 3H), 3.53 (m, 3H) 3.19 (s, 3H), 1.99 (m, 3H) ESI-MS *m/z* 518.6 (M + H⁺)⁺ MW: 518.43 g/mol. Mono-TFA salt FW: 632.42 g/mol.

Supplementary Material

Refer to Web version on PubMed Central for supplementary material.

Acknowledgement

This research was supported by National Institutes of Health grant AI070218.

Abbreviations

PFT, protein farnesyltransferase; 14DM, lanosterol 14 α -demethylase (CYP51); T cruzi, *Trypanosoma Cruzi*; IC₅₀, concentration of inhibitor resulting in 50% enzyme inhibition; EC₅₀, concentration of inhibitor resulting in 50% parasite growth inhibition; C_{max}, maximum plasma concentration; T_{max}, time to reach maximum plasma concentration; CYP3A4, cytochrome p450 3A4 (predominantly hepatic p450 enzyme).

References

1. Hucke O, Gelb MH, Verlinde CL, Buckner FS. The Protein Farnesyltransferase Inhibitor Tipifarnib as a New Lead for the Development of Drugs against Chagas Disease. *Journal of Medicinal Chemistry* 2005;48:5415–8. [PubMed: 16107140]
2. Sparreboom A, Marsh S, Mathijssen RH, Verweij J, McLeod HL. Pharmacogenetics of tipifarnib (R115777) transport and metabolism in cancer patients. *Investigational New Drugs* 2004;22:285–9. [PubMed: 15122075]
3. Zujewski J, Horak ID, Bol CJ, Woestenborghs R, Bowden C, End DW, Piotrovsky VK, Chiao J, Belly RT, Todd A, Kopp WC, Kohler DR, Chow C, Noone M, Hakim FT, Larkin G, Gress RE, Nussenblatt RB, Kremer AB, Cowan KH. Phase I and pharmacokinetic study of farnesyl protein transferase inhibitor R115777 in advanced cancer. *Journal of Clinical Oncology* 2000;18:927–941.
4. Venet M, End D, Angibaud P. Farnesyl protein transferase inhibitor ZARNESTRA R115777 - history of a discovery. *Current Topics in Medicinal Chemistry* 2003;3.
5. Molina J, Martins-Filho O, Brener Z, Romanha AJ, Loebenberg D, Urbina JA. Activities of the Triazole Derivative SCH 56592 (Posaconazole) against Drug-Resistant Strains of the Protozoan Parasite *Trypanosoma* (*Schizotrypanum*) *cruzi* in Immunocompetent and Immunosuppressed Murine Hosts. *Antimicrobial Agents and Chemotherapy* 2000;44:150–5. [PubMed: 10602737]
6. Bennett F, Saksena AK, Lovey RG, Liu Y, Patel NM, Pinto P, Pike R, Jao E, Girijavallabhan VM, Ganguly AK, Loebenberg D, Wang H, Cacciapuoti A, Moss E, Menzel F, Hare RS, Nomeir A. Hydroxylated analogues of the orally active broad spectrum antifungal, Sch 51048 (1), and the discovery of posaconazole [Sch 56592; 2 or (S,S)-5]. *Bioorganic and Medicinal Chemistry Letters* 2006;16:186–190. [PubMed: 16260134]
7. Saksena AK, Girijavallabhan VM, Wang H, Lovey RG, F. G, Mergelsberg I, Puar MS. Stereoselective Grignard additions to *N*-formyl hydrazones: a concise synthesis of NoxafilR side chain and a synthesis of NoxafilR. *Tetrahedron Letters* 2004;45:8249–8251.
8. Saksena, AK.; Girijavallabhan, VM.; Lovey, RG.; Pike, RE.; Wang, H.; Liu, Y.; Ganguly, AK.; Bennett, F. *Tetrahydrofuran Antifungals*. 1996. WO 1996/038443 A1

9. Reid TS, Beese LS. Crystal Structures of the Anticancer Clinical Candidates R115777 (Tipifarnib) and BMS-214662 Complexed with Protein Farnesyltransferase Suggest a Mechanism of FTI Selectivity. *Biochemistry* 2004;43:6877–6884. [PubMed: 15170324]
10. Podust LM, Poulos TL, Waterman MR. Crystal structure of cytochrome P450 14 α -sterol demethylase (CYP51) from *Mycobacterium tuberculosis* in complex with azole inhibitors. *Proceedings of the National Academy of Sciences* 2001;98:3068–3073.
11. Angibaud PR, Venet MG, Filliers W, Broeckx R, Ligny YA, Muller P, Poncelet VS, End DW. Synthesis Routes Towards the Farnesyl Protein Transferase Inhibitor ZARNESTRA. *European Journal of Organic Chemistry* 2004:479–486.
12. Frye SV, Johnson MC, Valvano NL. Synthesis of 2-aminobenzophenones via rapid halogen-lithium exchange in the presence of a 2-amino-N-methoxy-N-methylbenzamide. *Journal of Organic Chemistry* 1991;56:3750–3752.
13. Venet, MG.; Angibaud, PR.; Muller, P.; Sanz, GC. FARNESYL PROTEIN TRANSFERASE INHIBITING (IMIDAZOL-5-YL)METHYL-2-QUINOLINONE DERIVATIVES. 1997. WO 1997/021701 A1
14. Venet, MG.; Angibaud, PR.; Muller, P.; Sanz, GC. Farnesyl protein transferase inhibiting (imidazol-5-yl)methyl-2-quinolinone derivatives. 2000. US 6037350
15. Yang, BV. HETEROARYL-SUBSTITUTED QUINOLIN-2-ONE DERIVATIVES USEFUL AS ANTICANCER AGENT. 2000. WO 2000/047574 A1
16. Vejdeck Z, Holubek J, Ryska M, Koruna I, Svatek E, Budesinsky M, Protiva M. Reactions of 4-Chloro-1-nitrobenzene with o-substituted Phenylacetonitriles; Synthesis of 8-chloro-1-methyl(and methylthiomethyl)-6-(2-substituted phenyl)-4H-s-triazolo[4,3-a]-1,4-benzodiazepines. *Collection of Czech Chemical Communications* 1987;52:2545–2563.
17. Faller JW, Lavoie AR. Enantioselective Syntheses of Nonracemic Benzyl- α -d-Alcohols via Catalytic Transfer-Hydrogenation with Ru, Os, Rh, and Ir Catalysts. *Organometallics* 2002;21:3493–3495.
18. Mitchell RH, Lai Y. Syntheses and Reactions of the First Dithia[3.1.3.1]metacyclophanes, [2.1.2.1]Metacyclophanes, and [2.1.2.1]Metacyclophanes. *Journal of Organic Chemistry* 1984;49:2534–2540.
19. Friedman L, Shechter H. Preparation of Nitriles from Halides and Sodium Cyanide. An Advantageous Nucleophilic Displacement in Dimethyl Sulfoxide. *Journal of Organic Chemistry* 1960;25:877–9.
20. Walsh DA. The Synthesis of 2-Aminobenzophenones. *Synthesis* September;1980 1980:677–688.
21. Pratt EF, Draper JD. Reaction Rates by Distillation. I. The Etherification of Phenylcarbinols and the Transesterification of their Ethers. *Journal of the American Chemical Society* 1949;71:2846–2849.
22. Araujo MS, Martins-Filho OA, Pereira ME, Brener Z. A combination of benznidazole and ketoconazole enhances efficacy of chemotherapy of experimental Chagas' disease. *Journal of Antimicrobial Chemotherapy* 2000;45:819–824.
23. Brener Z, Cancado JR, Galvao LM, da Luz ZM, Filardi LS, Pereira ME, Santos LM, Cancado JR. An experimental and clinical assay with ketoconazole in the treatment of Chagas disease. *Memorias do Instituto Oswaldo Cruz* 1993;88:149–153. [PubMed: 8246750]
24. Bustamante JA, Bixby LM, Tarleton RL. Drug-induced cure drives conversion to a stable and protective CD8+ T central memory response in chronic Chagas disease. *Nature Medicine* 2008;14:542–550.
25. Corrales M, Cardozo R, Segura MA, Urbina JA, Basombrio MA. Comparative Efficacies of TAK-187, a Long-Lasting Ergosterol Biosynthesis Inhibitor, and Benznidazole in Preventing Cardiac Damage in a Murine Model of Chagas' Disease. *Antimicrobial Agents and Chemotherapy* 2005;49:1556–1560. [PubMed: 15793138]
26. Urbina JA, Payares G, Sanoja C, Lira R, Romanha AJ. In vitro and in vivo activities of ravuconazole on *Trypanosoma cruzi*, the causative agent of Chagas disease. *International Journal of Antimicrobial Agents* 2003;21:27–38. [PubMed: 12507835]
27. McMartin C, Bohacek RS. QXP: Powerful, rapid computer algorithms for structure-based drug design. *Journal of Computer-Aided Molecular Design* 1997;11:333–344. [PubMed: 9334900]
28. Yokoyama K, Zimmerman K, Scholten J, Gelb MH. Differential Prenyl Pyrophosphate Binding to Mammalian Protein Geranylgeranyltransferase-I and Protein Farnesyltransferase and Its Consequence on the Specificity of Protein Prenylation. *Journal of Biological Chemistry* 1997;272:3944–3952. [PubMed: 9020098]

29. Van Voorhis WC, Rivas KL, Bendale P, Nallan N, Horney C, Barrett LK, Bauer KD, Smart BP, Ankala S, Hucke O, Verlinde CLMJ, Chakrabarti D, Strickland C, Yokoyama K, Buckner FS, Hamilton AD, Williams DK, Lombardo LJ, Floyd D, Gelb MH. Efficacy, Pharmacokinetics, and Metabolism of Tetrahydroquinoline Inhibitors of Plasmodium falciparum Protein Farnesyltransferase. *Antimicrobial Agents and Chemotherapy* 2007;51:3659–3671. [PubMed: 17606674]
30. Buckner FS, Verlinde CL, La Flamme AC, Van Voorhis WC. Efficient technique for screening drugs for activity against *Trypanosoma cruzi* using parasites expressing beta-galactosidase. *Antimicrobial Agents and Chemotherapy* 1996;40:2592–7. [PubMed: 8913471]
31. Van Voorhis WC, Eisen H. Fl-160. A surface antigen of *Trypanosoma cruzi* that mimics mammalian nervous tissue. *Journal of Experimental Medicine* 1989;169:641–652. [PubMed: 2466939]

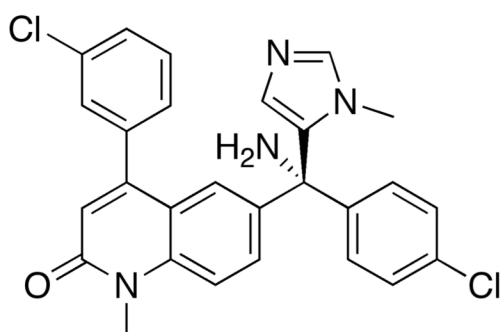
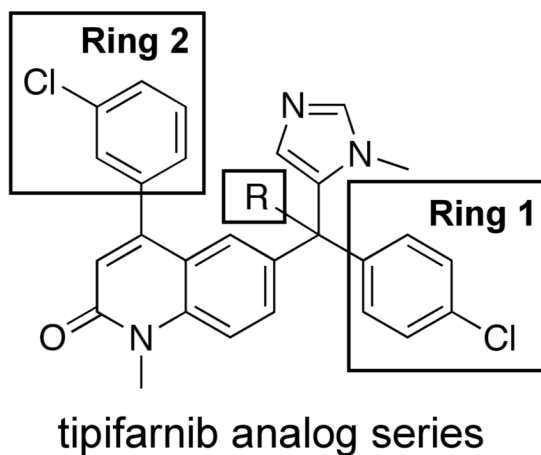
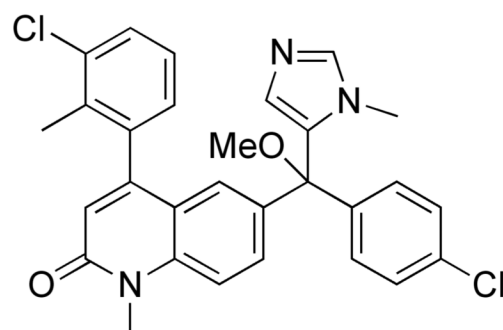
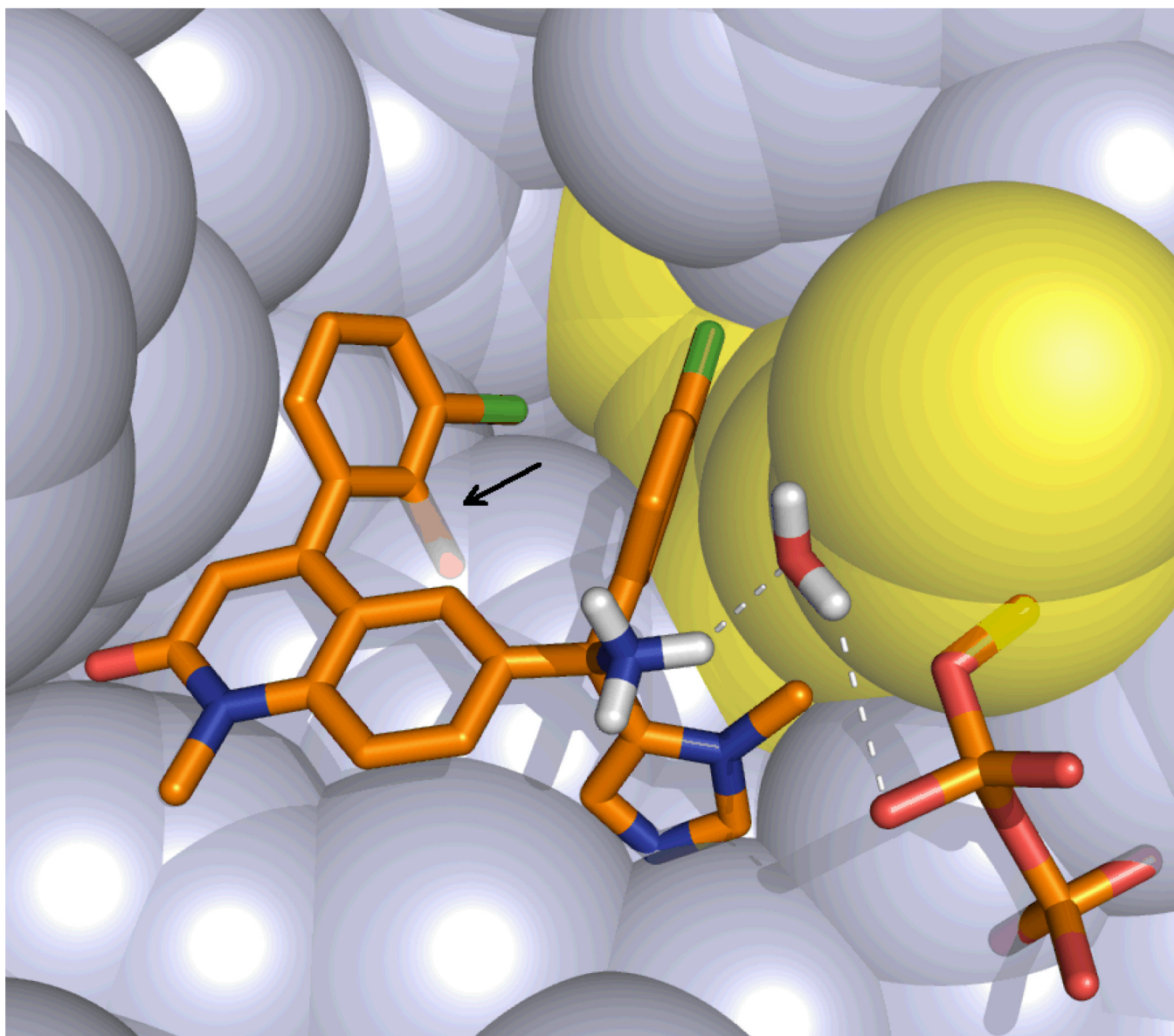
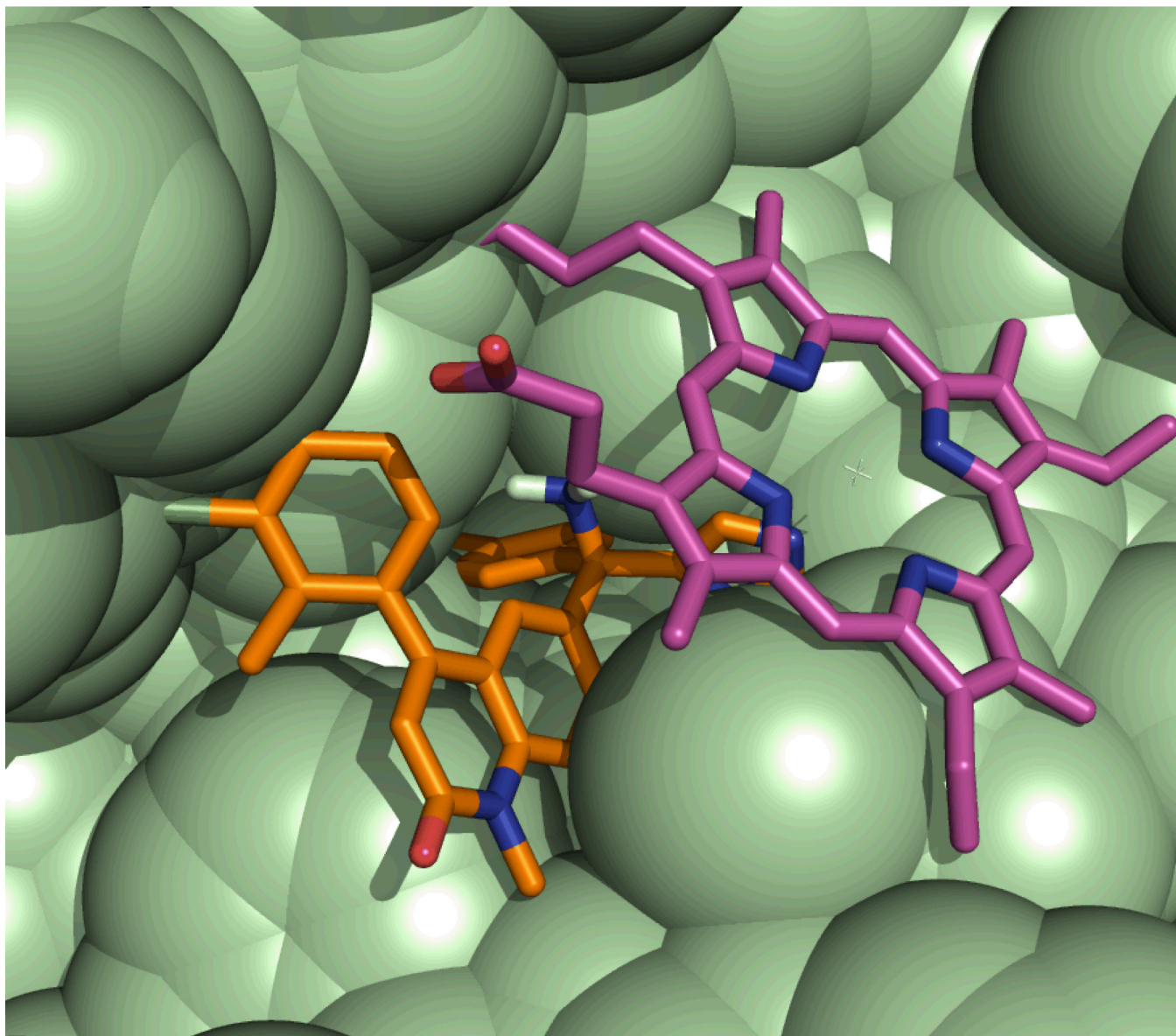
**1 tipifarnib** $T_c EC_{50} = 4 \text{ nM}$ $hPFT IC_{50} = 0.7 \text{ nM}$ **2g** $T_c EC_{50} = 0.6 \text{ nM}$ $hPFT IC_{50} = >5 \text{ } \mu\text{M}$

Figure I. Tipifarnib analog series ring numbering, tipifarnib and Compound **2g**.



**Figure II.**

(a) Mammalian PFT depicted with bound compound **2c**. Compound **2c** is depicted instead of the lead **2g** in order to show water-mediated hydrogen bonding between the ammonium group of tipifarnib or compound **2c** and the β -phosphate oxygen, which are shown in dotted lines. Compound **2c**, bridging water, and the diphosphate of farnesyl diphosphate are rendered as sticks. The prenyl chain is shown as yellow spheres. All van der Waal surfaces are displayed as doubled-radius surfaces to show ligand contacts. The superimposed arrow indicates the clash between the 2-methyl group of compound **2c** and the PFT surface. PFT α -subunit and residues R291 to K294 have been removed from the picture for clarity. (b) *T. cruzi* 14DM with bound compound **2c** and heme (both displayed as sticks) showing the accommodation of the inhibitor's 2-methyl group. An 11 Å sphere around the inhibitor is depicted and residues P93-N102, F103-T109 and F386-V406 removed from figure for clarity. All van der Waal surfaces are displayed as doubled-radius surfaces to show ligand contacts.

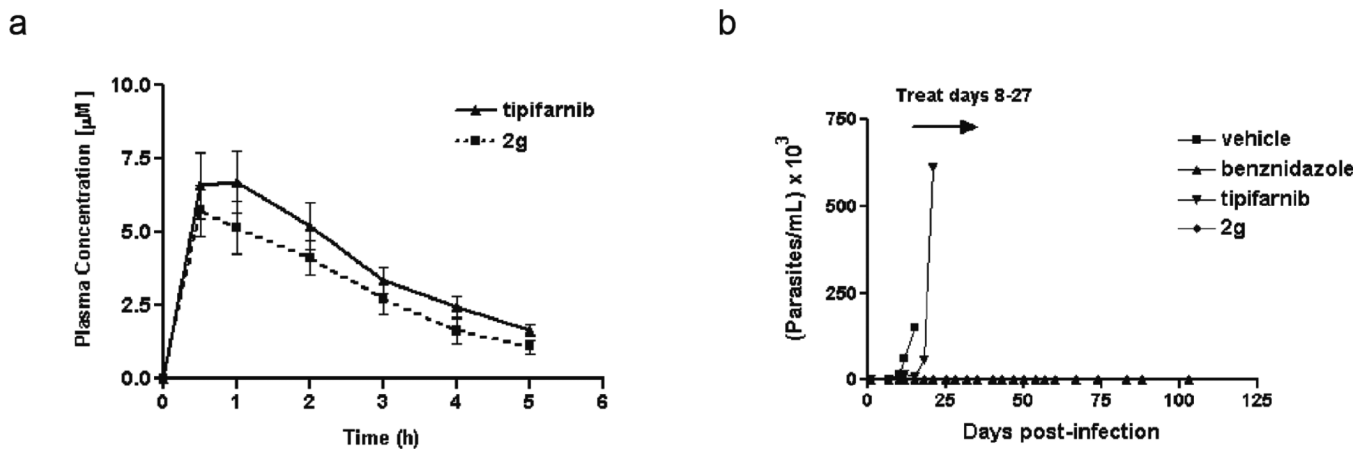
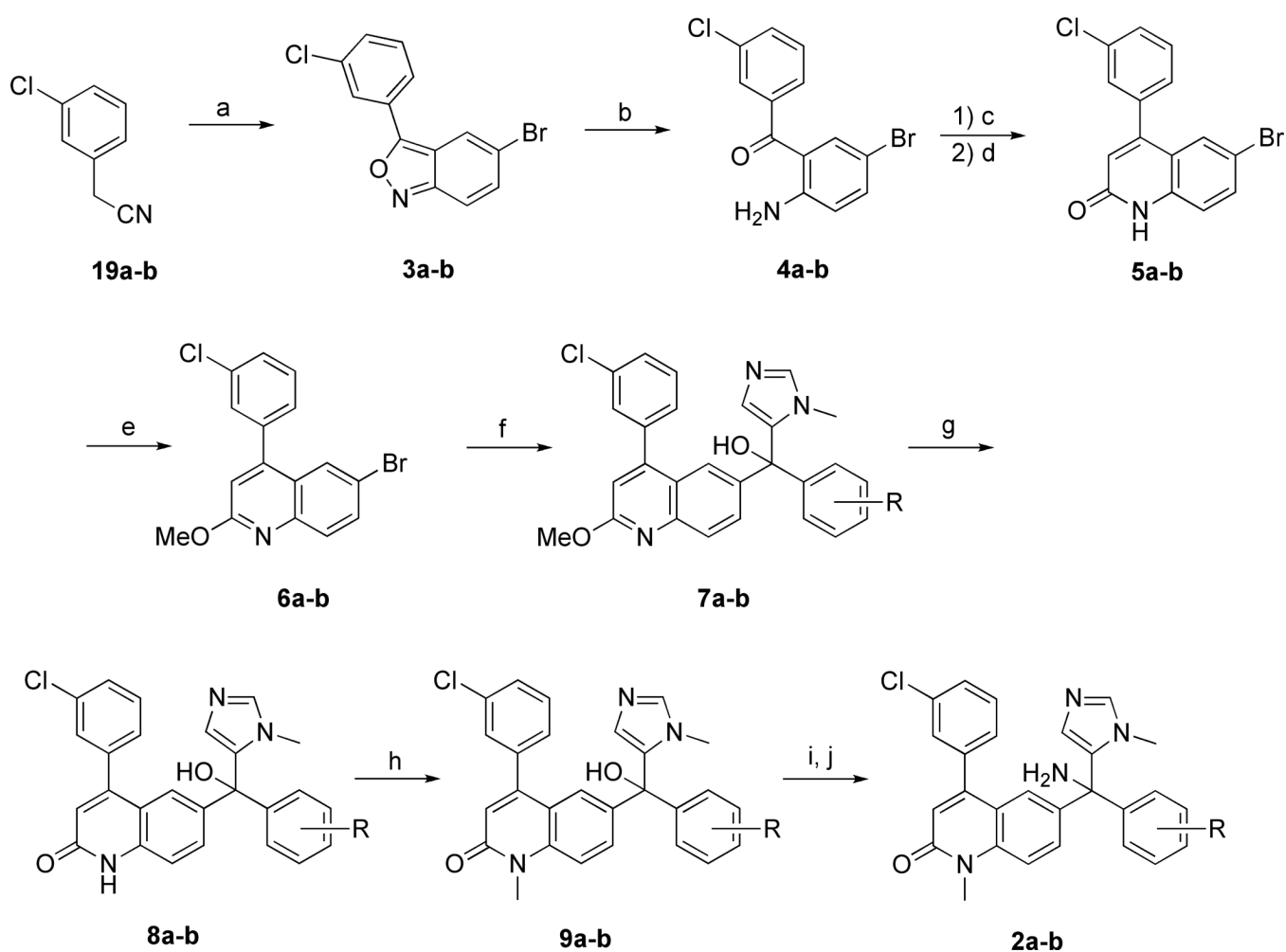


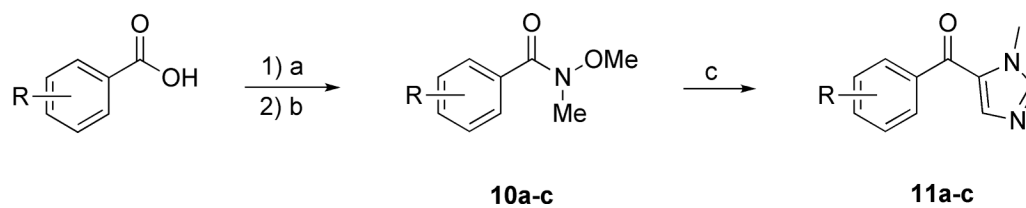
Figure III. Pharmacokinetics and efficacy of tipifarnib and 2g in mice

(a) Plasma levels were monitored following a single oral dose of 50 mg/kg in uninfected mice. Plotted values are an average of three mice for both tipifarnib and compound 2g. (b) Efficacy was monitored by measuring parasitemia in *T. cruzi* infected mice receiving treatment with tipifarnib (50 mg/kg twice daily), compound 2g (50 mg/kg twice daily), vehicle (twice per day), or benznidazole (100 mg/kg once daily). Treatments were administered by oral gavage for 20 consecutive days beginning on day 8 post-infection with *T. cruzi* trypomastigotes. Vehicle treated mice (negative control) were all dead by day 16 post-infection.



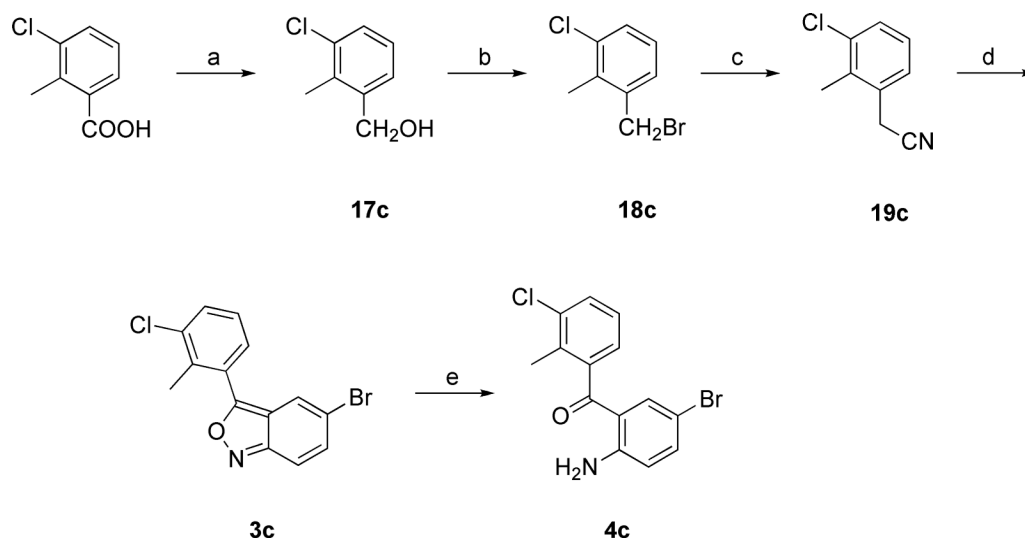
Scheme Ia. Synthesis of Tipifarnib Analogs from Phenylacetonitrile

a) p-bromonitrobenzene, NaOH, MeOH, **10–50%** b) TiCl_3 , $\text{H}_2\text{O}/\text{THF}$, rt **62%** c) Ac_2O , toluene, reflux d) t-BuOK, DME 20 °C, **66%** (2 steps) e) BF_4OMe_3 , DCM, **63%** f) i.) n-BuLi, THF, -78 °C ii. (**11a-b**) **60%** g) 6N HCl, THF, reflux 6 hr **60%** h) CH_3I , NaOH, BTEAC, THF, rt **66%** i) SOCl_2 , neat, 12 hrs j) NH_3 , THF, rt **52%** (2 steps)



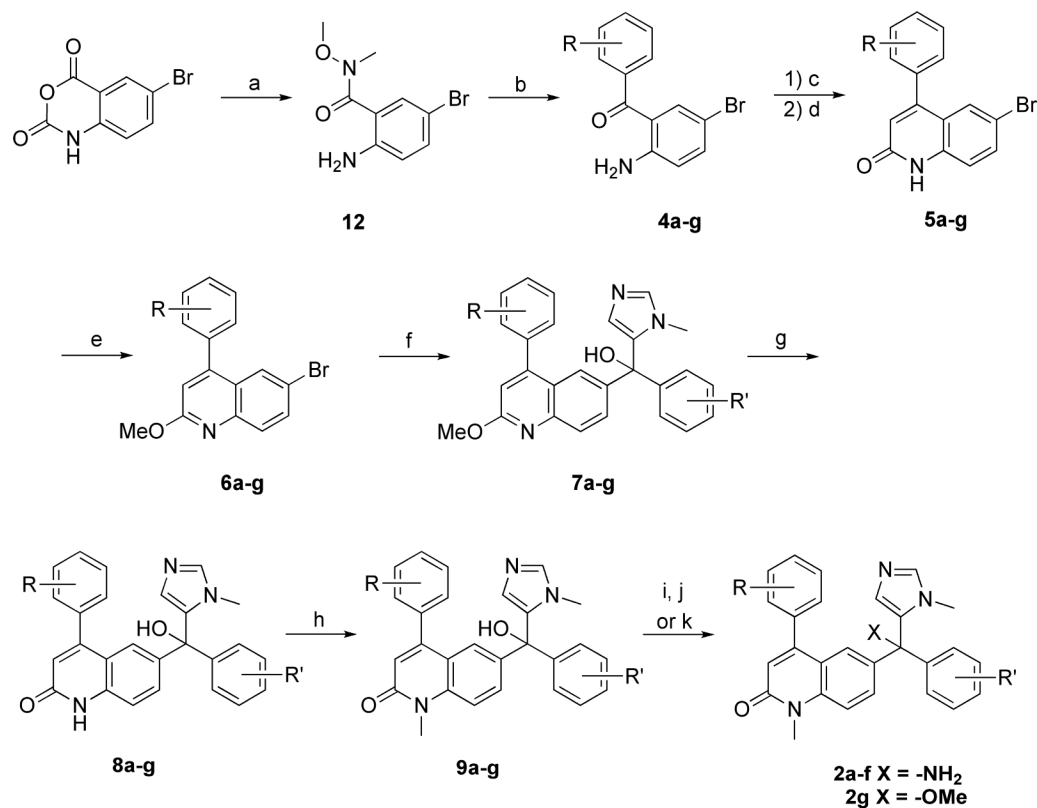
Scheme Ib. Synthesis of (Imidazol-5-yl)phenylmethanone Intermediate (11)

a) SOCl_2 , neat, rt b) $\text{CH}_3\text{ONHCH}_3$, pyridine, DCM, **90%** (2 steps) c) *N*-methylimidazole, i.) $n\text{-BuLi}$, THF, -78°C ii.) Et_3SiCl , -78°C iii.) $n\text{-BuLi}$, THF, -78°C , **77%**



Scheme II. Synthesis of 3-Chloro-2-methylphenylacetonitrile Intermediate

a) LAH, THF, **quant.** b) PBr_3 , DCM, **90%** c) NaCN, DMSO, **85%** d) p-BrPhNO₂, NaOH, MeOH, **10%** e) TiCl_3 , H₂O/THF, rt, **50%** (**4% overall**)



Scheme III. Synthesis of Tipifarnib Analogs from 5-Bromoisatoic anhydride

a) CH₃ONHCH₃ HCl, pyridine, DCM, **83%** b) RPhBr (2eq.), n-butyllithium (2eq.), THF, **85%** c) Ac₂O, toluene, reflux d) t-BuOK, DME 20 °C, **66%** (2 steps) e) BF₄OMe₃, DCM, **63%** f) i.) n-BuLi, THF, -78 °C ii. (**11a-c**), **60%** g) 6N HCl, THF, reflux, **60%** h) CH₃I, NaOH, BTEAC, THF, rt, **66%** i) SOCl₂, neat, 12 hrs j) NH₃, THF, rt, **52%** (2steps) k) tosic acid (1eq + cat.), MeOH, reflux, **75%**.

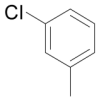
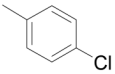
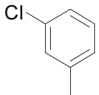
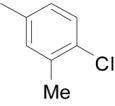
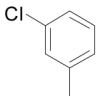
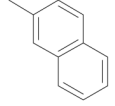
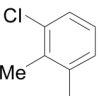
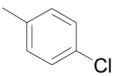
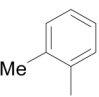
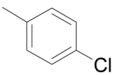
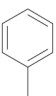
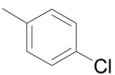
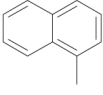
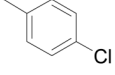
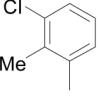
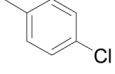
Compound	Ring 2	Ring 1	R
1			-NH₂
2a			-NH₂
2b			-NH₂
2c			-NH₂
2d			-NH₂
2e			-NH₂
2f			-NH₂
2g			-OMe

Chart I.
Structures of Tipifarnib **1** and Tipifarnib analogs **2a-g**.

Table I

In vitro test results of tipifarnib and other compounds. (Numbers are averages of duplicate or triplicate determinations).

Compound	Mammalian PFT IC50 (nM)	<i>T. cruzi</i> amastigote EC50 (nM)	Ratio IC50/EC50	CYP3A4 IC50 (nM)
Tipifarnib	0.7	6	0.1	1700
2a	13	23	0.2	-
2b	17	45	0.4	-
2c	294	21	14	1300
2d	300	23	13	1350
2e	4	12	0.3	-
2f	485	22	230	550
2g	>5000*	0.6	>7700*	870
Ketoconazole	-	0.3	-	40
Posaconazole	-	0.3	-	350

* Compound **2g** was evaluated up to 5 μ M, displaying less than 50% inhibition at this concentration.